Physiology-Based Face Recognition in the Thermal Infrared Spectrum

Pradeep Buddharaju, Ioannis T. Pavlidis, *Senior Member, IEEE*, Panagiotis Tsiamyrtzis, and Mike Bazakos

Abstract—The current dominant approaches to face recognition rely on facial characteristics that are on or over the skin. Some of these characteristics have low permanency can be altered, and their phenomenology varies significantly with environmental factors (e.g., lighting). Many methodologies have been developed to address these problems to various degrees. However, the current framework of face recognition research has a potential weakness due to its very nature. We present a novel framework for face recognition based on physiological information. The motivation behind this effort is to capitalize on the permanency of innate characteristics that are under the skin. To establish feasibility, we propose a specific methodology to capture facial physiological patterns using the bioheat information contained in thermal imagery. First, the algorithm delineates the human face from the background using the Bayesian framework. Then, it localizes the superficial blood vessel network using image morphology. The extracted vascular network produces contour shapes that are characteristic to each individual. The branching points of the skeletonized vascular network are referred to as Thermal Minutia Points (TMPs) and constitute the feature database. To render the method robust to facial pose variations, we collect for each subject to be stored in the database five different pose images (center, midleft profile, left profile, midright profile, and right profile). During the classification stage, the algorithm first estimates the pose of the test image. Then, it matches the local and global TMP structures extracted from the test image with those of the corresponding pose images in the database. We have conducted experiments on a multipose database of thermal facial images collected in our laboratory, as well as on the time-gap database of the University of Notre Dame. The good experimental results show that the proposed methodology has merit, especially with respect to the problem of low permanence over time. More importantly, the results demonstrate the feasibility of the physiological framework in face recognition and open the way for further methodological and experimental research in the area.

Index Terms—Face recognition, biometrics, physiology, thermal infrared, vascular network.

1 Introduction

Biometrics has received a lot of attention during the last few years—both from the academic and business communities. It has emerged as a preferred alternative to traditional forms of identification, like card IDs, which are not embedded into one's physical characteristics. Research in several biometric modalities including face, fingerprint, iris, and retina recognition has produced varying degrees of success [1]. Face recognition stands as the most appealing modality, since it is the natural mode of identification among humans and is totally unobtrusive. At the same time, however, it is one of the most challenging modalities [2].

Research in face recognition has been biased toward the visible spectrum for a variety of reasons. Among those is the availability and low cost of visible band cameras and the undeniable fact that face recognition is one of the primary activities of the human visual system. Machine recognition of human faces, however, has proven more problematic than the seemingly effortless face recognition performed by humans. The major culprit is light variability, which is prevalent in the visible spectrum due to the reflective nature of incident light in this band. Secondary problems are associated with the difficulty of detecting facial disguises [3].

Recently, researchers have investigated the use of near-infrared (near-IR) imagery for face recognition with good results [4], [5], [6]. Near-IR imagery like visible imagery is formed from reflected radiation. Therefore, the imaging process still requires an external source of illumination. The added advantage with respect to visibility is that the eye is not sensitive in this range, and illumination can be used in a more flexible and possibly covert manner.

As a solution to the aforementioned problems, researchers have started investigating the use of thermal IR for face recognition purposes [7], [8], [9]. However, many of these research efforts in thermal face recognition use the thermal IR band only as a way to see in the dark or reduce the deleterious effect of light variability [10], [11]. Methodologically, they do not differ very much from face recognition algorithms in the visible band, which can be classified as appearance-based [12], [13] and feature-based approaches [14], [15]. Recently, attempts have been made to fuse the visible and IR modalities to increase the performance of face recognition [16], [17], [18], [19], [20], [21].

In this paper, we present a novel approach to the problem of thermal facial recognition that realizes the full potential of the thermal IR band. It consists of a statistical face segmentation and a physiological feature extraction

- *P. Buddharaju and I.T. Pavlidis are with the Department of Computer Science, University of Houston, 501 Philip G. Hoffman, Houston, TX 77204. E-mail: braju@cs.uh.edu, ipavlidi@central.uh.edu.*
- *P. Tsiamyrtzis is with the Department of Statistics, Athens University of Economics and Business, 76 Patission Street, 10434 Athens, Greece. E-mail: pt@aueb.gr.*
- *M. Bazakos is with the Honeywell Technology Center, 3660 Technology Dr., Minneapolis, MN 55418. E-mail: Mike.Bazakos@Honeywell.com.*

Manuscript received 6 Feb. 2006; revised 24 July 2006; accepted 6 Nov. 2006; published online 18 Jan. 2007.
Recommended for acceptance by S. Prabhakar, J. Kittler, D. Maltoni, L. O'Gorman, and T. Tan.
For information on obtaining reprints of this article, please send e-mail to: tpami@computer.org and reference IEEECS Log Number TPAMISI-0126-0206.
Digital Object Identifier no. 10.1109/TPAMI.2007.1007.

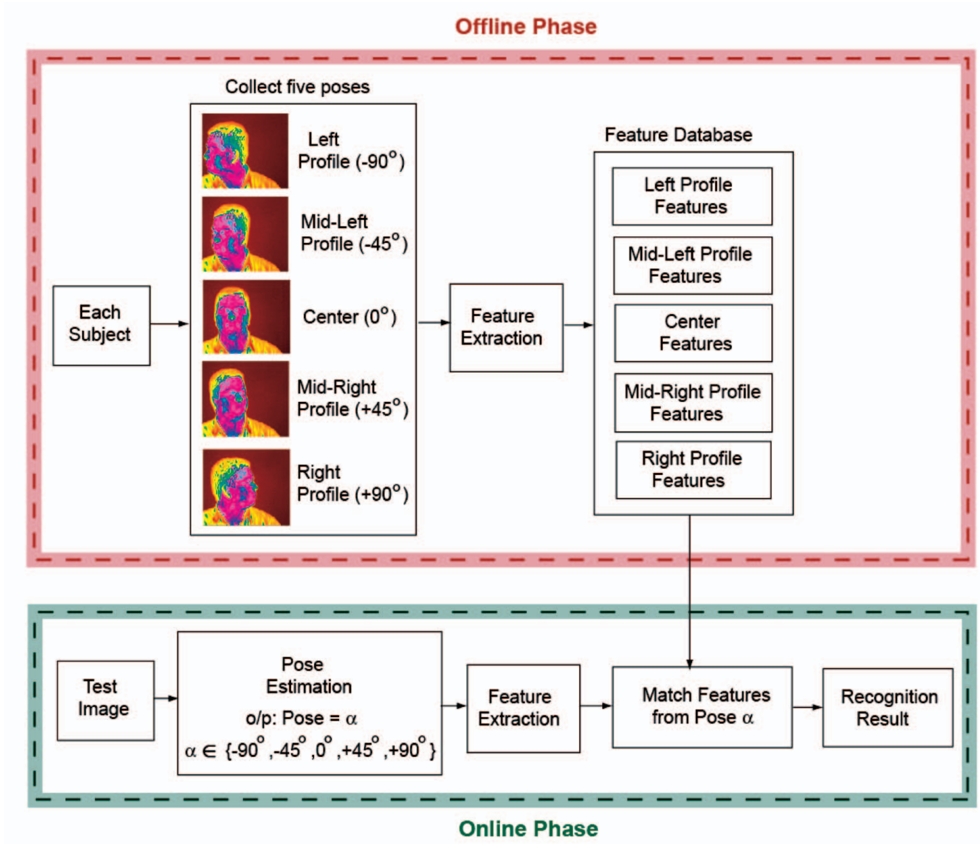

Fig. 1. Architecture of our face recognition methodology.

algorithm tailored to thermal phenomenology. The physiological vector is formed from the thermal imprint of the facial vascular network. The closest work to our research is the use of hand vein structure for human identification [22], [23]. This is done typically through active near-IR sensing and is not a standoff modality, as it requires close proximity to the sensor and the subject's cooperation.

Prokoski and Riedel [24] anticipated the possibility of extracting the vascular network from thermal facial images and using it as a feature space for face recognition. However, they did not present an algorithmic approach for achieving this. To the best of our knowledge, this is the first attempt to develop a face recognition system using physiological information on the face. Our aim is to promote a different way of thinking about face recognition in thermal IR, which carries distinct advantages when compared with other modalities. An early stage of this research was reported briefly in the *Proceedings of the 2005 IEEE Conference on Advanced Video and Signal-Based Surveillance* [25]. A follow-up version, where the pose estimation component was added, appeared in the *Workshop Proceedings of the 2006 Conference on Computer Vision and Pattern Recognition* [26].

Fig. 1 shows the architecture of the proposed methodology. The goal of face recognition is to match a query face image against a database of facial images to establish the identity of an individual. Our system operates in the following two phases to achieve this goal:

1. **Offline phase**. The thermal facial images are captured by an IR camera. For each subject to be stored in the database, we record five different poses. A two-step segmentation algorithm is applied on each pose image to extract the vascular network from the face. Thermal Minutia Points (TMPs) are detected on the branching points of the vascular network and stored in the database (see Fig. 1).
2. **Online phase**. Given a query image, TMPs of its vascular network are extracted and matched against those of the corresponding pose images stored in the database (see Fig. 1).

In the following sections, we will describe our face recognition methodology and its performance in detail. In Section 2, we present the vascular feature extraction algorithm. In Section 3, we discuss the vascular network matching algorithm. In Section 4, we present the experimental results and attempt a critical evaluation. We conclude the paper in Section 5.

2 Vascular Feature Extraction

2.1 Uniqueness

A thermal IR camera with good sensitivity provides the ability to image indirectly superficial blood vessels on the human face [28]. The convective heat transfer effect from the flow of "hot" arterial blood in superficial vessels creates characteristic thermal imprints, which are at a gradient with the surrounding tissue. The pattern of the underlying blood vessels (and the corresponding thermal imprints) is quite complex (see Fig. 2). The question is if this complex pattern is characteristic to each individual and can serve as a useful biometric signature.

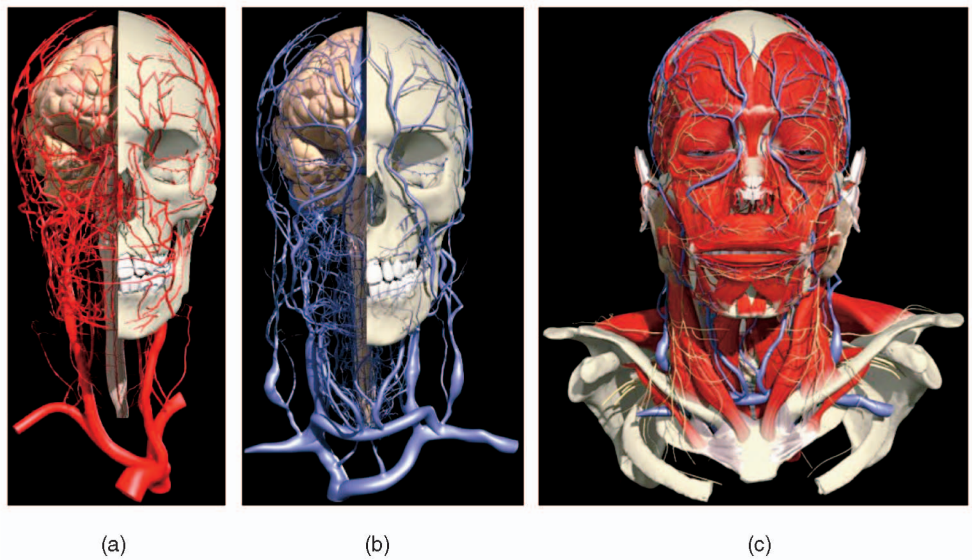

Fig. 2. Generic map of superficial blood vessels on the face, courtesy of Primal Pictures [27]. (a) Overview of an arterial network. (b) Overview of a venous network. (c) Arteries and veins together underneath the surface of the facial skin.

In the area of medicine, some very interesting work was conducted regarding the uniqueness of the facial vascular network. The primary motivation behind this line of research was the localization of anatomical features for reconstructive surgery purposes. For example, Pinar and Govsa [29] conducted extensive research on the anatomy of the Superficial Temporal Artery (STA) and its branches. They studied the STA anatomy in 27 subjects. Among other things, they found that the bifurcation point of STA (see Fig. 3) was above the zygomatic arch in only 20 out of the 27 samples. In six samples, the bifurcation was exactly over the arch and, in one sample, there was no bifurcation at all. Further variability was observed in the STA branches. Specifically, in one sample, double parietal branches were observed. In 21 samples, zygomatico-orbital arteries ran towards the face, parallel to the zygomatic arch, and distributed in the orbicularis oculi muscle. One has to take into account that STA is only one major facial vessel among many. Assuming that such variability is typical to other facial vessels and branches, their combination is bound to produce a very characteristic pattern for each individual.

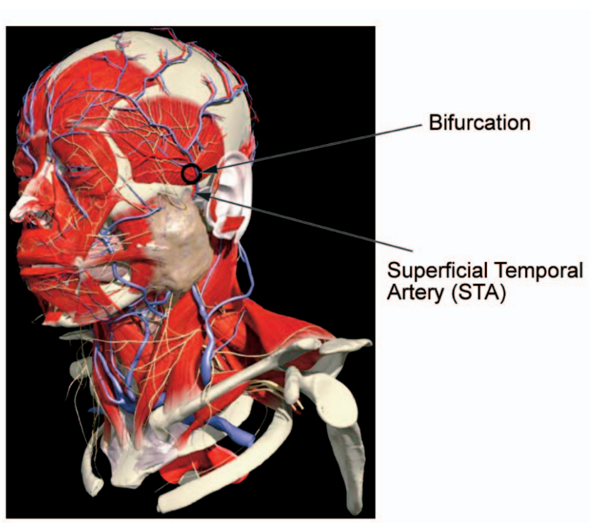

Fig. 3. Example of the STA and its bifurcation around the zygomatic arch, courtesy of Primal Pictures [27]. Clinical studies have established its highly variable topology across individuals.

In another study, medical researchers found implicit evidence of uniqueness of the cutaneous vasculature in the high variability of reflex drives [30].

In addition, one has to take into account that the proposed face recognition method does not depend only on the topology of the facial vascular network but also on the fat depositions and skin complexion. The reason is that imagery is formed by the thermal imprints of the vessels and not the vessels directly. Even if the vessel topology was absolutely the same across individuals, still, the thermal imprints would differ due to variable absorption from different fat padding (skinny faces versus puffy faces) [31] and variable heat conductance from different skin complexion (dark skin is less conductive).

Besides the medical evidence, which appears to be strong, and the supporting heat transfer principles, the "uniqueness" of the facial vascular network is also reinforced by experimental investigation. This paper presents good classification results on a proprietary database (University of Houston) as well as a publicly available database (University of Notre Dame [32]). Such experimental investigations constitute the main "proof of uniqueness" in other biometric modalities (e.g., fingerprint recognition [33]), and of course, they gain more weight as the size of the databases increases. In the case of thermal facial vessel imprints, the size of the databases is still relatively small, yet statistically significant (several hundred samples). One particular example that makes a very strong case for "uniqueness" is the discovery of different thermal facial vessel imprints even in identical twins [24].

In the last few years, one relevant biometric that has gained acceptance is the venous structure at the back of the hand. It is imaged typically with active near-IR light, and the image is formed due to backscattering. The claim of "uniqueness" is based primarily on experimental evidence from database classification efforts. No substantial medical

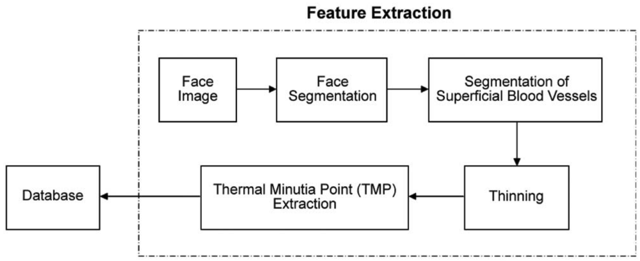

Fig. 4. Architecture of feature extraction algorithm.

research was pursued on the uniqueness of the hand's venous structure, as reconstructive hand surgery is not as prevalent as facial surgery. In addition, the venous network at the back of the hand is not nearly as complicated as the facial vessel network (see Fig. 2). Yet, it is increasingly accepted as a legitimate biometric [22] and is used in practice [23] based mainly on experimental evidence from database classification efforts.

Hence, evidence from medical research and reasoning based on heat transfer principles suggest that the facial vessel network is characteristic to each individual. This educated guess has been verified by our classification results in databases of nontrivial size (see Section 4). Fig. 4 outlines the architecture of our feature extraction algorithm. It is a case of staged abstraction whereby information is reduced from the full image to the face, to the vascular network, and to its bifurcation points (TMPs). These three major stages of feature extraction are described in some detail in Sections 2.2-2.4.

2.2 Face Segmentation

Due to its physiology, a human face consists of "hot" parts that correspond to tissue areas that are rich in vasculature and "cold" parts that correspond to tissue areas with sparse vasculature. This casts the human face as a bimodal temperature distribution entity, which can be modeled using a mixture of two normal distributions. Similarly, the background can be described by a bimodal temperature distribution with walls being the "cold" objects and the upper part of the subject's body dressed in cloths being the "hot" object. The consistency of bimodality across subjects and image backgrounds is striking. We approach the problem of delineating facial tissue from the background by using a Bayesian framework since we have a priori knowledge of the bimodal nature of the scene. We first reported our facial tissue segmentation algorithm in [25], [34], where the interested reader may find more details.

Fig. 5b visualizes the result of our Bayesian segmentation scheme on the subject shown in Fig. 5a. Part of the subject's nose has been erroneously classified as the background, and a couple of cloth patches from the subject's shirt have been erroneously marked as facial skin. This is due to occasional overlapping between portions of the skin and background distributions. The isolated nature of these mislabeled patches makes them easily correctable through postprocessing. We apply a three-step postprocessing algorithm on the binary segmented image. Using foreground (and background) correction, we find the mislabeled pixels in the foreground (and background) and reassign them. Fig. 5c visualizes the result of postprocessing, where all the segmentation imperfections have been eliminated.

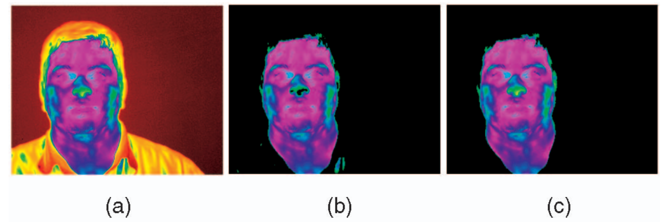

Fig. 5. Segmentation of facial skin region. (a) Original thermal facial image. (b) Result of Bayesian segmentation, where background is depicted in black. (c) Result of postprocessing.

2.3 Segmentation of Superficial Blood Vessels

Once a face is delineated from the rest of the scene, the segmentation of superficial blood vessels from the facial tissue is carried out in the following steps [28], [34]:

Step 1. Process the image to reduce noise and enhance the edges.

Step 2. Apply morphological operations to localize the superficial vasculature.

In a thermal imagery of human tissue, the major blood vessels have weak sigmoid edges. This is due to the natural phenomenon of heat diffusion, which entails that when two objects with different temperatures are in contact (e.g., vessel and the surrounding tissue), heat conduction creates a smooth temperature gradient at the common boundary [35]. These weak sigmoid edges can be handled effectively by using anisotropic diffusion. The anisotropic diffusion filter is formulated as a process that enhances object boundaries by performing intraregion as opposed to interregion smoothing. One can visualize this clearer in an area with sparser vasculature than that of the face. Fig. 6 shows vividly how the application of anisotropic diffusion on the thermal image of a wrist enhanced the sigmoid edges around the vessel and, at the same time, helped to remove the noise formed due to hair.

The mathematical equation that describes this process is

$$\frac{\partial I(\bar{x},t)}{\partial t} = \nabla(c(\bar{x},t)\nabla I(\bar{x},t)). \tag{1}$$

In our case, $\mathrm{I}(\bar{x},t)$ is the thermal IR image, $\bar{x}$ refers to the spatial dimensions, and t refers to time. $\mathrm{c}(\bar{x},t)$ is called the diffusion function. The discrete version of the anisotropic diffusion filter of (1) is given as follows:

$$\begin{aligned} I_{t+1}(x,y) = I_t + \frac{1}{4} * \big[&c_{N,t}(x,y)\nabla I_{N,t}(x,y) \\ &+ c_{S,t}(x,y)\nabla I_{S,t}(x,y) + c_{E,t}(x,y)\nabla I_{E,t}(x,y) \\ &+ c_{W,t}(x,y)\nabla I_{W,t}(x,y)\big]. \end{aligned} \tag{2}$$

The four diffusion coefficients and four gradients in (2) correspond to four directions (that is, north, south, east, and west) with respect to the location (x,y). Each diffusion coefficient and the corresponding gradient are calculated in the same manner. For example, the coefficient along the north direction is calculated as follows:

$$c_{N,t}(x,y) = \exp\left(\frac{-\nabla I^2_{N,t}(x,y)}{k^2}\right), \tag{3}$$

where $I_{N,t} = I_t(x,y+1) - I_t(x,y)$.

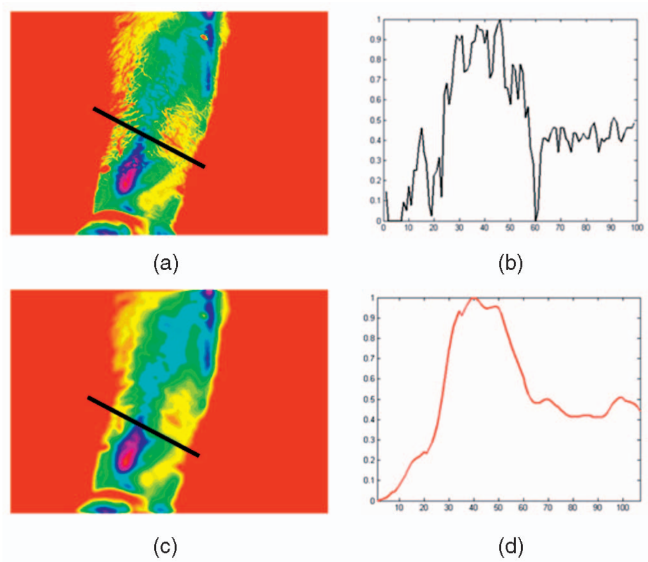

Fig. 6. Anisotropic diffusion on the thermal image of a human wrist. (a) Segmented wrist image. (b) Profile of the line drawn across the segmented image (shown in black color in (a)). (c) Result of applying anisotropic diffusion on (a). (d) Profile of the same line drawn across diffused image (shown in black color in (b)).

Image morphology is then applied on the diffused image to extract the blood vessels that are at a relatively low contrast compared to that of the surrounding tissue. We employ, for this purpose, a top hat segmentation method, which is a combination of erosion and dilation operations. Top hat segmentation takes on two forms: the white top hat segmentation that enhances the bright objects in the image and the black top hat segmentation that enhances dark objects. In our case, we are interested in the white top hat segmentation because it helps to enhance the bright ("hot") ridgelike structures corresponding to the blood vessels. In this method, the original image is first opened, and then, this opened image is subtracted from the original image:

$$\begin{aligned} I_{open} &= (I \ominus S) \oplus S, \\ I_{top} &= I - I_{open}, \end{aligned} \tag{4}$$

where I, I_{open}, and I_{top} are the original, opened, and white top hat segmented images, respectively, S is the structuring element, and $\ominus$ and $\oplus$ are the morphological erosion and dilation operations, respectively. Fig. 7b depicts the result of applying anisotropic diffusion to the segmented facial tissue shown in Fig. 7a, and Fig. 7c shows the corresponding vascular network extracted via white top hat segmentation.

2.4 Extraction of Thermal Minuta Points

The extracted blood vessel contours differ between subjects. We call the branching points of the blood vessel contours TMPs. TMPs can be extracted from the network of blood vessel contours in ways similar to those used for fingerprint minutia extraction. A number of methods have been proposed [36] for robust and efficient extraction of minutia from fingerprint images. Most of these algorithms describe each minutia point by at least three attributes, including its type, its location in the fingerprint image, and the local ridge orientation. We adopt a similar approach for extracting TMPs from vascular networks. Specifically, our TMP extraction algorithm proceeds as follows:

1. It estimates the local orientation of the vascular network.
2. It skeletonizes the vascular network.
3. It extracts the TMPs from the thinned vascular network.
4. It removes the spurious TMPs.

We define the local orientation function $\Psi(x, y)$ as the angle formed between any blood vessel contour and the horizontal axis at each pixel (x, y) of the image. This orientation function provides the basis for capturing the overall pattern of the vascular network. We adapt the approach proposed in [37] to compute the orientation function on the vascular network image.

Next, our algorithm thins the vascular contours down to a one-pixel thickness (skeleton) [38]. Each pixel in the thinned map is assigned a value of 1 if it is on the vessel and 0 if it is not. Considering 8-neighborhood $(N_0, N_1, \ldots, N_7)$ around each pixel, a pixel (x, y) is marked as TMP if $(\sum_{i=0}^{7} N_i) > 2$ (see Fig. 8).

The last step of the TMP extraction algorithm is the removal of spurious TMPs. These spurious TMPs are the result of imperfections in segmentation and the preceding image processing. They are of two types: clustered TMPs and spikes formed from trivially short branches (see Fig. 9). Such spurious TMPs, if left, will affect seriously the performance of the pattern recognition algorithm.

Based on our experimentation, the vascular network of a typical facial image contains between 50 and 80 legitimate TMPs. The location (x, y) and corresponding orientation function $\Psi(x, y)$ of the cleaned TMP set is stored in the database. Fig. 10 shows the results of each stage of the feature extraction algorithm on a thermal facial image.

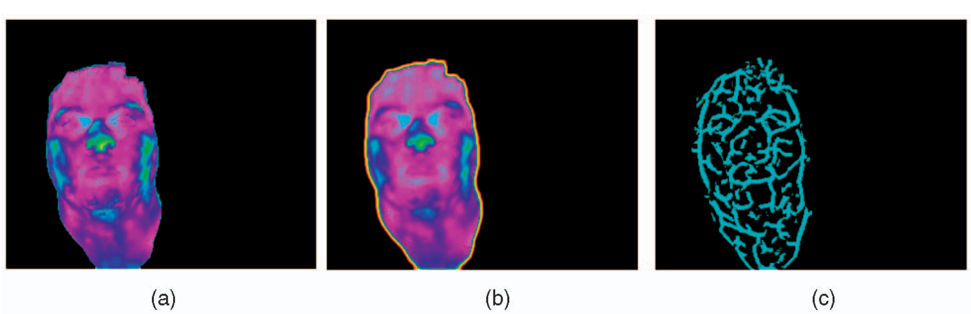

Fig. 7. Vascular network extraction. (a) Original segmented image. (b) Anisotropically diffused image. (c) Blood vessels extracted using white top hat segmentation.

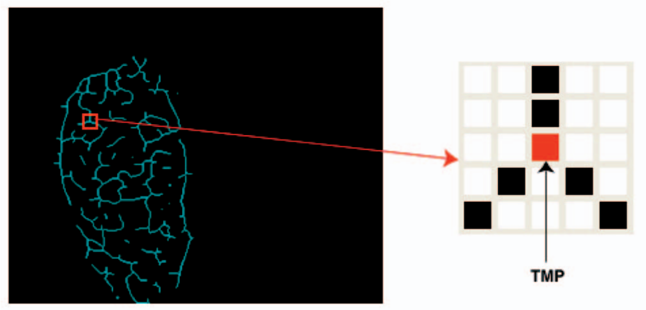

Fig. 8. A Thermal Minuta Points extracted from the thinned vascular network.

3 Matching

Each subject's record in the database consists of five different poses to account for pose variation during the testing phase. Since facial images from the same person look quite different across multiple views, it is very important that the search space includes facial images with a pose similar to the pose of the test image. Given a test image, we first estimate its pose. Then, the task is simply to match the TMP network extracted from the test image against the TMP database corresponding to the estimated pose.

3.1 Estimation of Facial Pose

To the best of our knowledge, this is the first time that the issue of pose estimation in thermal facial imagery is addressed. However, as it is the case with face recognition in general, a number of efforts have been made to address the issue of facial pose estimation in visible band imagery [39], [40]. We adapt the algorithm proposed in [39] for estimating head pose in thermal IR imagery. Specifically, we select a random subset from our thermal facial data set and apply Principal Component Analysis (PCA) to reduce the dimensionality of the image vector. The training set includes all five pose images for a number of subjects. Images from the training set are not used in either gallery or probe sets introduced in Section 4 so that the matching algorithm is not biased. Fig. 11 illustrates sample face images from our training set across multiple views. Then, we train the Support Vector Machine (SVM) classifier with the PCA vectors of face samples. Given a probe image, SVM can classify it against one of the five poses (center, midleft profile, left profile, midright profile, and right profile) under consideration.

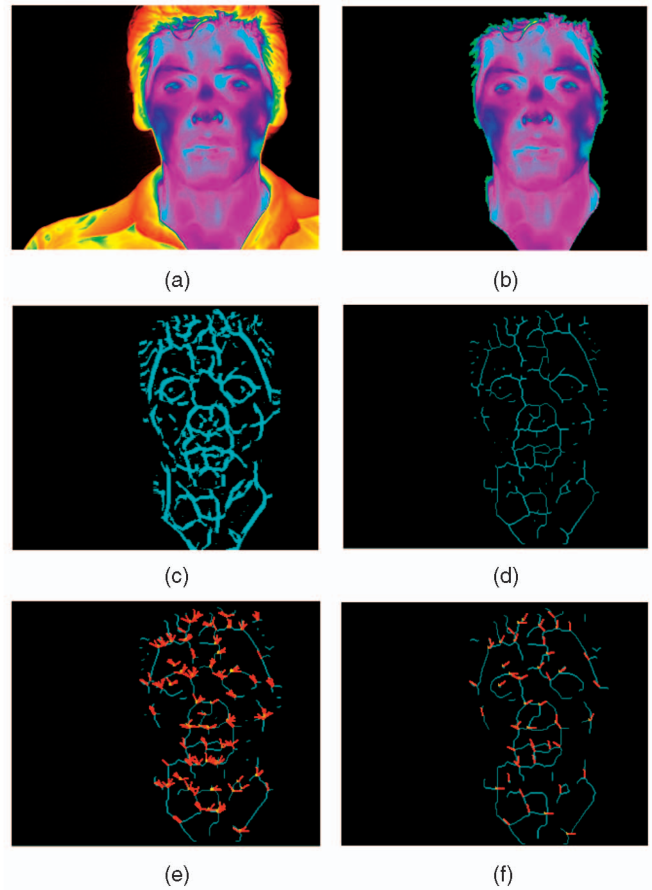

Fig. 10. Visualization of the various stages of the vascular feature extraction algorithm. (a) A typical thermal facial image. (b) Facial tissue delineated from the background. (c) A network of vascular contours extracted from the thermal facial image. (d) A skeletonized vessel map. (e) Extracted TMPs from branching points. (f) A cleaned TMP set.

3.2 Matching of Thermal Minuta Points

Numerous methods have been proposed for matching fingerprint minutiae, most of which try to simulate the way forensic experts compare fingerprints [36]. Popular techniques are alignment-based point pattern matching, local structure matching, and global structure matching. Local minutiae-matching algorithms are fast, simple, and more tolerant to distortions. Global minutiae-matching algorithms feature high distinctiveness. A few hybrid approaches have been proposed, where the advantages of both local and global methods are exploited [41], [42]. We

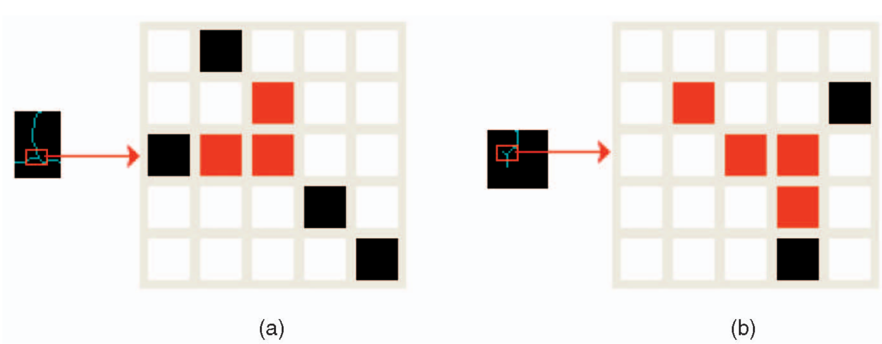

Fig. 9. Spurious TMPs. (a) Clustered TMPs. (b) Spikes formed due to a trivially short branch.

Fig. 11. Samples from our training set featuring five different poses per subject. From left to right, the views depicted are given as follows: left profile, midleft profile, center, midright profile, and right profile.

have adapted the hybrid method proposed in [41] to perform TMP matching.

For each TMP $M(x, y, \Psi)$ that is extracted from the vascular network, we consider its N nearest neighbor TMPs $M(x_n, y_n, \Psi_n)$, $n = 1, \ldots, N$. Then, the TMP $M(x, y, \Psi)$ can be characterized by a new feature vector:

$$L_M = \{\{d_1, \varphi_1, \vartheta_1\}, \{d_2, \varphi_2, \vartheta_2\}, \ldots, \{d_N, \varphi_N, \vartheta_N\}, \Psi\}, \quad (5)$$

where

$$\begin{aligned} d_n &= \sqrt{(x_n - x)^2 + (y_n - y)^2}, \\ \varphi_n &= diff(\Psi_n, \Psi), \\ \vartheta_n &= diff\left(\arctan\left(\frac{y_n - y}{x_n - x}\right), \Psi\right) \end{aligned} \quad (6)$$

for $n = 1, 2, \ldots, N$. d_n is the euclidean distance of TMP $M(x, y, \Psi)$ from its nth neighbor. The function $diff()$ calculates the difference of two angles and scales the result within the range $[0, 2\pi)$. Given a test image $\mathbf{I_t}$, the feature vector of each of its TMPs is compared with the feature vector of each TMP of a database image with a compatible pose. Two TMPs M and M' are marked as a matched pair if the minimum absolute difference between corresponding features $\{\delta_d^{min}, \delta_\varphi^{min}, \delta_\vartheta^{min}, \delta_\Psi\}$ is less than the specific threshold values $\{T_d, T_\varphi, T_\vartheta, T_\Psi\}$. The threshold values are chosen in a way that accommodates linear deformations and translations. The final matching score between the test and a database image is given as follows:

$$Score = \frac{NUM_{match}}{\max\{NUM_{test}, NUM_{database}\}}, \quad (7)$$

where NUM_{match} represents the number of matched TMP pairs, and NUM_{test} and $NUM_{database}$ represent the number of TMPs in the test and database images, respectively. If the highest matching score between the test and database images is greater than a specific threshold, the corresponding database image is classified as a confident match. If not, the match is considered weak, and the classifier concludes that the subject does not have a record in the database.

4 Experimental Results

4.1 Experiments on the University of Houston Database

To evaluate our method, we built a data set of thermal facial images from volunteers of different sex, race, and age groups. The data set consists of 7,590 thermal facial images from 138 subjects (55 images per subject) with varying poses and facial expressions. Five images from each subject (each image representing one of the five training poses) were used in the gallery set. From these gallery images, we extracted TMPs and stored them in the database. The remaining 50 images per subject at arbitrary poses were included in the probe set to test the performance of our algorithm.

All images were recorded in two separate data gathering efforts about six months apart. Each individual data gathering effort lasted a few days with multiple recordings. Unfortunately, only a small portion of the original population participated in the second data gathering effort. Therefore, for most subjects, the extracted testing images are from the initial data gathering effort only. For the few subjects (4 out of 138) for whom we have recordings from data gathering efforts spaced six months apart, the probe image set is composed half from the initial session and half from the latter session. The gallery set is composed of images strictly from the initial session. The performance of the method was excellent for those four subjects with multimonth samples, but of course,

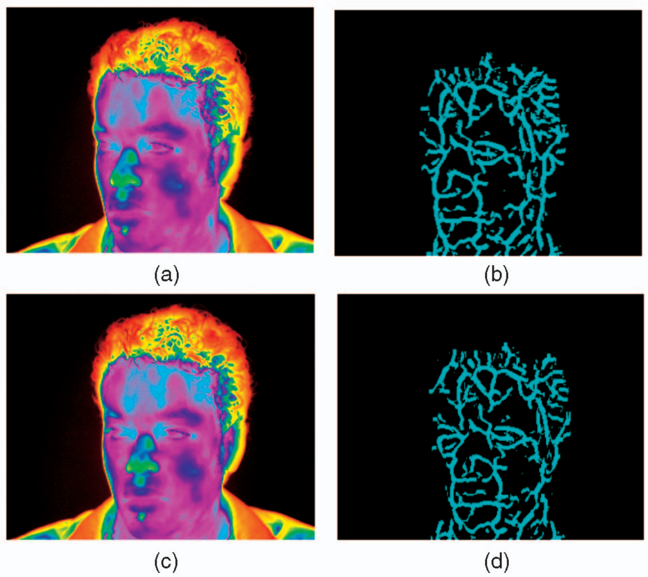

Fig. 12. (a) A test image and (b) its corresponding vascular network. (c) A midleft profile image picked from the training database by pose estimation and (d) its corresponding vascular network.

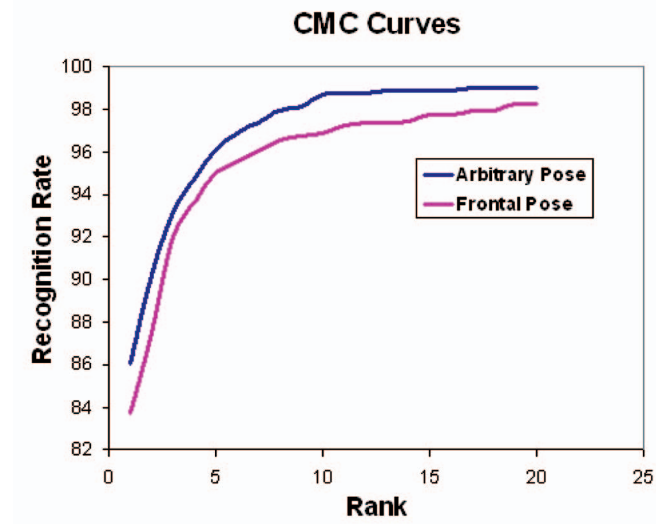

Fig. 13. CMC curves of our method for the frontal and arbitrary pose experiments.

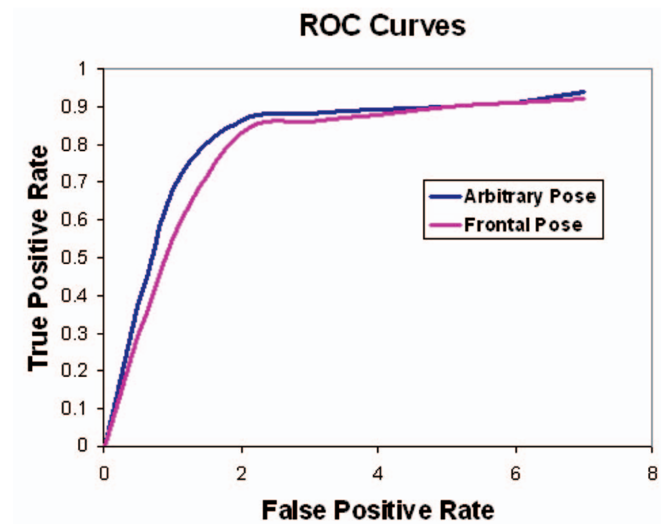

Fig. 14. ROC curves of our method for the frontal and arbitrary pose experiments.

the small size of the set did not allow generalizations regarding the issue of feature permanence.

The images were captured using a high-quality Mid-Wave Infrared (MWIR) camera produced by Flir Systems (Phoenix model) [43]. The camera features a Focal Plane Array (FPA) made out of InSb and is 640×512 pixels large. It is sensitive in the 3.0-5.0 $\mu\mathrm{m}$ spectral range and has a Noise Equivalent Temperature Difference (NEDT) of $0.01^{\circ}\mathrm{C}$. The camera was outfitted with a 50 mm MWIR lens also from Flir Systems.

Many 2D face recognition algorithms that perform well on frontal image data sets often have problems when tested on images with arbitrary poses [2]. Our face recognition algorithm overcomes this problem by using multiple pose images in gallery, which allows pose invariance in the probe image. We found experimentally that the five poses we included in the gallery set of our face recognition algorithm are sufficient to accommodate yaw rotations (including tilt rotations to a certain extent). As shown in Fig. 12, when a probe that is close to the midleft profile is queried, pose estimation correctly picks the corresponding mid-left profile image from the gallery data set to perform matching. The small variation in the pose that exists between the probe and gallery images might cause minor position and angle differences in the corresponding TMP networks. This can be compensated by choosing appropriate values for thresholds $\{T_d, T_\varphi, T_\vartheta, \text{ and } T_\Psi\}$ as discussed in Section 3.2.

We conducted two experiments on the University of Houston database to evaluate the performance of our face recognition method. In the first experiment, we took into account only frontal pose images. Specifically, we constrained the probe set to images with poses between the midleft and midright profiles. This probe set was matched against frontal images in the database. In the second experiment, we used the entire probe set, which includes images from all five poses and variations in between. This probe set was matched against the full database galleries that contains five pose images per subject. Figs. 13 and 14 show the results of the two experiments. Specifically, Fig. 13 shows the Cumulative Math Characteristic (CMC) curves of the two experiments, and Fig. 14 shows the Receiver Operating Characteristic (ROC) curves based on various threshold values for the matching score discussed in Section 3.2.

First, one can observe that our face recognition method performs better in the arbitrary pose experiment rather than the frontal pose experiment. This is to be expected, as test cases close to the midleft and midright profiles in the first experiment may be lost, since only frontal database images are being used for matching. In the second experiment, more poses are at play, but also much finer gradation of pose images in the database galleries.

Second, the results demonstrate the promise, as well as some problems with our methodology. The CMC curve shows that rank 1 recognition is over 86 percent, and rank 5 recognition is over 96 percent. This performance puts a brand-new approach close to the performance of mature visible band recognition methods. In contrast, the ROC curve reveals a weakness of the current method, as it requires a False Acceptance Rate (FAR) over 20 percent to reach a

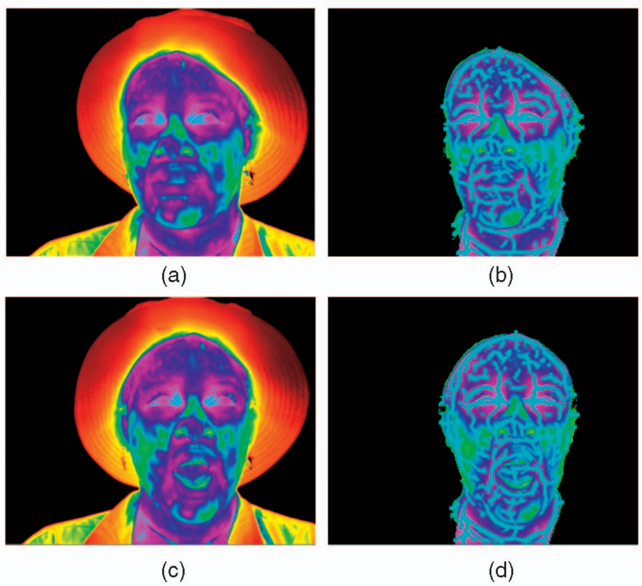

Fig. 15. (a) A probe image and (b) its corresponding vascular network (overlaid over the segmented image). (c) A gallery image of the same subject exhibiting large facial expression and (d) its corresponding vascular network (overlaid over the segmented image). Nonlinear vascular deformations are apparent in the mandible area.

positive acceptance rate above the 86 percent range. To address this problem, we believe that we need to estimate and eliminate the incorrect TMPs, as well as nonlinear deformations in the extracted vascular network caused due to large facial expressions, and nonlinear pose transformations. Fig. 15 shows an example of nonlinear deformations caused in the vascular network between gallery and probe images of the same subject due to pose and facial expression changes. Even though the matching algorithm described in Section 3.2 works fine with linear transformations in the vascular network, it affords a small latitude in the case of nonlinear transformations.

4.2 Experiments on the University of Notre Dame Database—Low-Permanence Problem

A major challenge associated with thermal face recognition is the recognition performance over time [44]. Facial thermograms may change, depending on the physical condition of the subject. This renders difficult the task of acquiring similar features for the same person over time. Previous face recognition methods in thermal IR that use direct temperature data reported degraded performance over time [13], [20]. However, our method attempts to solve this problem by extracting facial physiological information to build its feature space. This information is not only characteristic to each person, but also remains relatively invariant to physical conditions. Although, the thermal facial maps of the same subject appear to shift, the vascular network is more resistant to change. In imaging terms, the contrast between the temperatures in the vascular pixels and the surrounding pixels is relatively invariant, albeit the absolute temperature values shift appreciably. This is a direct consequence of the thermoregulatory mechanism of the human body. Our morphological image processing simply capitalizes upon this phenomenon and extracts the invariant vascular contours out of the variable facial thermal maps.

Due to the small number of subjects in the University of Houston database, for which we had images spread over several months, no statistically significant quantification of the low-permanence problem was possible. For this reason, we obtained permission to apply the method on the database of the University of Notre Dame [32]. This database has a large collection of facial images acquired from both visible and long-wave IR cameras. They held acquisitions weekly, and most of the subjects in the database participated multiple times.

In more detail, the database consists of 2,294 images acquired from 63 subjects during nine different sessions under specific lighting and expression conditions. The spatial resolution of the images is 312×239 pixels (about half of that featured in the University of Houston database). They used three lights during data collection: one located at the center approximately 8 feet in front of the subject, one at 4 feet to the right, and one at 4 feet to the left of the subject. The subjects were asked to provide two expressions during acquisition—"neutral" and "smiling." The database is divided into four different gallery and probe sets using the Feret style naming convention [45]:

1. LF (central light turned off) + FA (neutral expression),
2. LF (central light turned off) + FB (smiling expression),
3. LM (all three lights on) + FA (neutral expression), and
4. LM (all three lights on) + FB (smiling expression).

The database also contains an exclusive training set (different from the gallery and probe sets) with samples collected from several subjects, from which a face space can be constructed for the PCA recognition algorithm. We did not use this training set, since our algorithm is feature-based and, hence, does not require any explicit training. However, each of the gallery sets (say, LF-FA) can be tested against the other three probe sets (say, LF-FB, LM-FA, and LM-FB). This way, we tested our algorithm on 12 different pairs of gallery and probe sets. In each of these experiments, the gallery set had one image per subject, and the probe set had several disjoint images per subject, depending on how many different acquisition sessions the subject attended. Fig. 16 shows a sample of the gallery and probe images of a subject from the University of Notre Dame database.

The authors of the University of Notre Dame database compared the performance of face recognition in visible and IR modalities from both same-session and time-gap data sets [20], [13]. They used a PCA-based face recognition algorithm for these studies. They found that both visible and IR modalities performed well on same-session experiments, and none of them is significantly better than the other. However, in time-lapse experiments, they found that the PCA-based recognition using IR images had poor performance. This is an expected outcome, since PCA is an appearance-based face recognition algorithm that directly uses temperature values to project the query image onto face space. The thermal facial map may be different between gallery and probe images depending on the ambient and physical conditions, which may cause the PCA algorithm to fail.

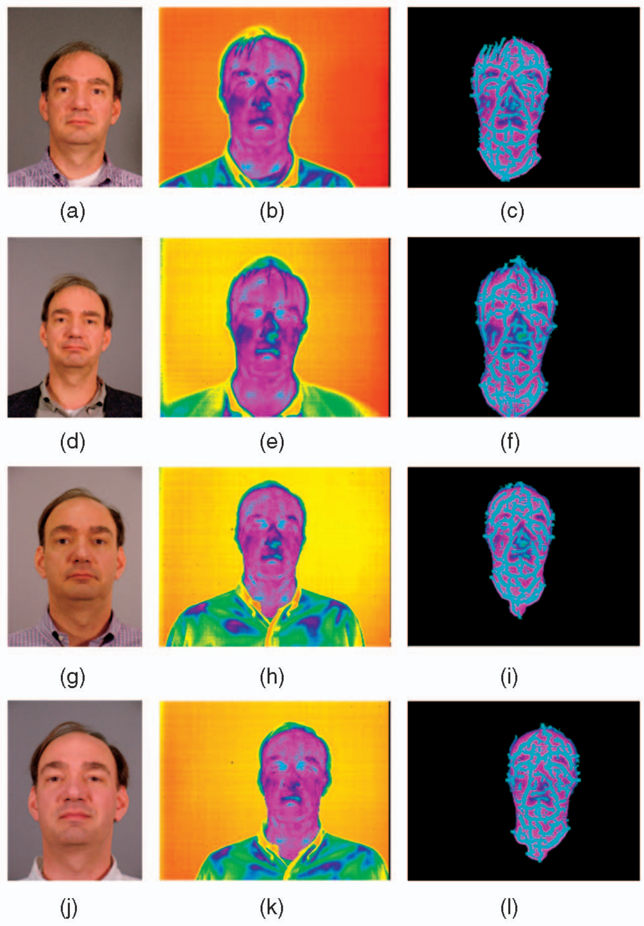

Fig. 16. Sample images of a subject in the University of Notre Dame database. The images were acquired over the span of several months. (a) Visible images (not used here). (b) Corresponding thermal IR images. Differences in the thermal facial maps can be visually appreciated. (c) Vascular annotation after the application of our feature extraction algorithm.

We compared the performance of our method with a PCA-based recognition algorithm to test the robustness of features extracted from the facial vascular network. Table 1 summarizes the rank 1 recognition results using our algorithm versus the PCA algorithm on each of the 12 possible experiments. Each entry in the left column of Table 1 corresponds to a gallery set, and each entry in the top row corresponds to a probe set. From the results, it can be clearly seen that our method yields better recognition results despite the presence of time and temperature variations inherent in this database. This is a clear indication that by abstracting away the thermal facial map to a physiological feature vector, the low-permanence problem can be addressed more adequately.

4.3 Parameter Optimization

The proposed face recognition method depends on the selection of several threshold values. To rationalize the choice of these threshold values and optimize performance, we pursued sensitivity analysis. First, we investigated optimal values for T_d, T_ϕ, and T_θ, which are the distance and orientation thresholds regulating the matching of corresponding minutia points (see Section 3.2). We selected two facial thermal images for 20 subjects. For each of these

TABLE 1
Rank 1 Recognition Performance of Our Algorithm (University of Houston) versus the PCA Algorithm on Each of the 12 Experiments on the University of Notre Dame Database

	Probe			
Gallery	FA—LF	FA—LM	FB—LF	FB—LM
FA—LF	-	82.65% (UH)	80.77% (UH)	81.33% (UH)
	-	78.74% (PCA)	76.83% (PCA)	75.77% (PCA)
FA—LM	81.46% (UH)	-	79.38% (UH)	80.25% (UH)
	79.23% (PCA)	-	75.22% (PCA)	73.56% (PCA)
FB—LF	80.27% (UH)	81.92% (UH)	-	80.56% (UH)
	74.88% (PCA)	76.57% (PCA)	-	74.23% (PCA)
FB—LM	80.67% (UH)	82.25% (UH)	79.46% (UH)	-
	69.56% (PCA)	74.58% (PCA)	78.33% (PCA)	-

subjects, we manually labeled the matching minutia pairs between the corresponding images, as depicted in Fig. 17. Fig. 18 shows the resulting graphs. We chose as an optimal threshold value a number that is barely greater than the vast majority of the values given by the sample individual pairs. In all three cases, this corresponds to separating relatively compact clusters from small sets of outliers. Based on this experimental analysis, we found that the optimal minutia matching thresholds are $T_d = 10$, $T_\phi = 30$, and $T_\theta = 70$.

As we explained in Section 3.2, a total matching score is computed based on the number of accepted (after threshold) matching minutia pairs. This computation repeats for all possible matches between the incoming image and the database images. The database image that scores the highest is the candidate recognition result. This result is admissible only if it is greater than a threshold value T_{score}. Otherwise, the recognition is considered iffy, and it is discarded. We determined the optimal value of T_{score} based on the Equal Error Rate (ERR). This is the rate at which both FAR and False Rejection Rate (FRR) are equal. To find the ERR, we used 500 thermal facial images from 50 subjects (10 images per subject). Fig. 19 shows the FAR and FRR curves for different values of T_{score}. As can be seen in Fig. 19, the system has EER at $T_{score} = 65$.

4.4 Operational Limitations

Major operational limitations to the current feature extraction method fall into the following two categories:

1. Glasses are opaque in the thermal IR spectrum; hence, they block important vascular information in the periorbital area. Also, thick facial hair (for example, beard) reduces significantly the radiation emitted from the surface of the skin and may cause failure, even at the face segmentation stage. Fig. 20 shows examples of face segmentation where parts of the face containing glasses and hair are segmented out.
2. The robustness of the method degrades when there is substantial perspiration. This results in a highly nonlinear shift of the thermal map that alters

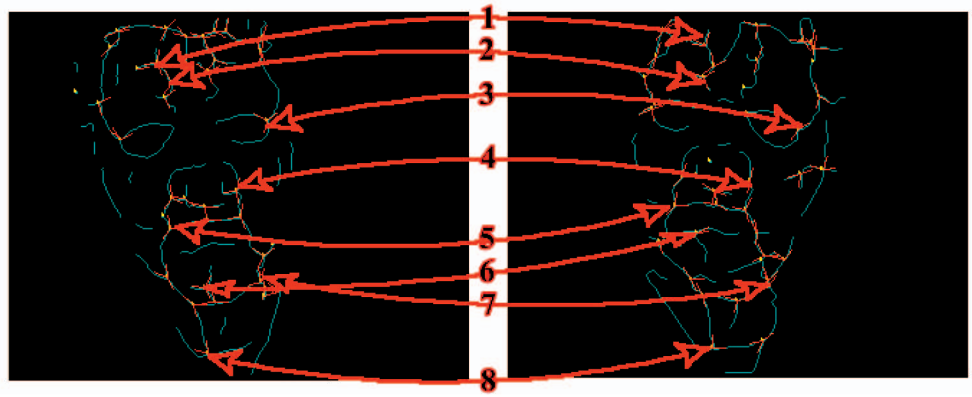

Fig. 17. Selection of matching minutia pairs from two images of the same subject.

radically the radiation profile of the face. For the moment, this should be considered as the operational limit of the method. A practical scenario where such a case may arise is when a subject is imaged after a strenuous exercise that lasted several minutes. Another possible breakdown may arise when the subject remains in a very hot environment, heavily dressed, for a substantial amount of time.

We have performed an experiment whereby a subject is imaged at the following instances:

- in a baseline condition (Fig. 21a),
- after 1 min of rigorous walking (Fig. 21c),
- after 5 min of rigorous walking (Fig. 21e), and
- after 5 min of rigorous jogging (Fig. 21g).

The second column of Fig. 21 shows the corresponding vessel extraction results. In Fig. 21c, the metabolic rate of the subject shifted to higher gear, but perspiration is still not a major problem. One can find evidence of the higher metabolic rate by looking at the left temporal area, where the region around the rich vasculature has become deeper cyan (hotter) in Fig. 21c with respect to Fig. 21a. This is an example of a positive linear shift (warming up), which the vessel extraction algorithm handles quite well (see Fig. 21d versus Fig. 21b). As the exercise becomes more strenuous and lasts longer, perspiration increases and introduces a negative nonlinear shift (cooling down) in the thermal map. This is especially pronounced in the forehead, where most of the perspiration pores are. Due to this, some unwanted noise starts creeping in the vascular map in Fig. 21f, which becomes more dramatic in Fig. 21h. The performance of the vessel extraction algorithm deteriorates, but not uniformly. For example, the vessel extraction algorithm continues to perform quite well in the cheeks, where perspiration pores are sparse, and the cooling down effect is not heavily nonlinear. In contrast, performance is a lot worse in the forehead area, where some spurious vessel contours are introduced due to severe nonlinearity in the thermal map shift.

The deterioration of the performance of the feature extraction algorithm has direct bearing on the performance of the matching algorithm. Specifically, for the vascular network in Fig. 21d, the matching score is 83 percent, which guarantees correct recognition despite the shift in the thermal map. For the vascular network in Fig. 21b, the matching score falls to 77 percent, which makes correct recognition ambivalent. Finally, for the vascular network in Fig. 21h, the matching score becomes 56 percent, which makes correct recognition impossible.

5 Conclusions

We have outlined a novel approach to the problem of face recognition in thermal IR. The cornerstone of the approach is the use of characteristic and time-invariant physiological information to construct the feature space.

Although thermal facial maps shift over time, the contrast between the superficial vasculature and surrounding tissue remains invariant. This physiological feature has permanence and is very difficult to be altered (under the skin). Therefore, it gives a potent advantage to any face recognition method that may use it.

We designed a method that represents the first attempt to realize this physiological framework for face recognition. Our main goal was to establish the feasibility and assess the promise of the overall concept. Since our method is 2D, we pay particular attention to neutralize the adverse effect of pose variability in the matching process. Specifically, our method proceeds as follows: First, it separates the facial tissue from the background by using a novel Bayesian segmentation algorithm. Second, it extracts the vascular contour network from the surface of the skin by using white top hat segmentation preceded by anisotropic diffusion. Third, it localizes the TMPs in the vascular network and uses them as the basis of a feature vector. Fourth, it performs recognition by matching TMP-based feature vectors. Our method borrows some ideas from fingerprint recognition, since the vascular network appears to have phenomenological similarities with the ridge network.

The most important conclusion of our research so far, is that physiology-based face recognition appears to be feasible and have potential, especially as a way of addressing the issue of low permanence over time. The current method has some weak points, which, if they are being cured, may propel physiology-based face recognition to outstanding performance. Specifically, the current methodology lacks a rigorous quality control mechanism when it comes to extraction of vascular contours. Truly, most of the contours appear to be at places where superficial vasculature is expected (e.g., carotid

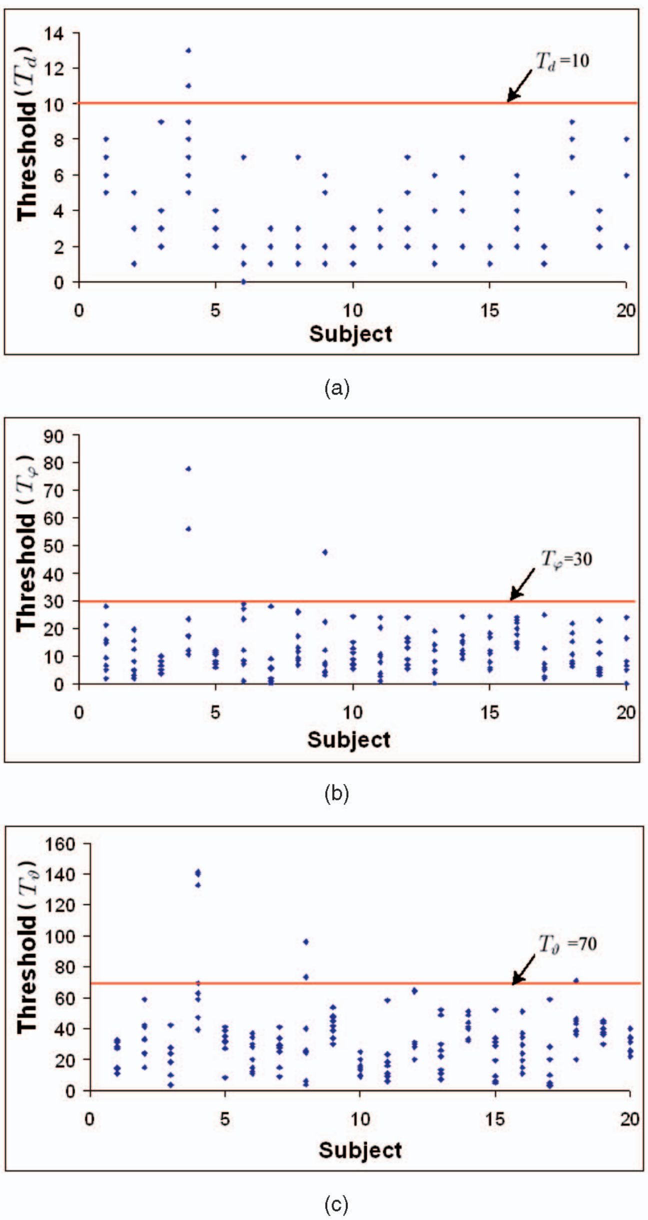

Fig. 18. Threshold values for selected minutia pairs for each subject.

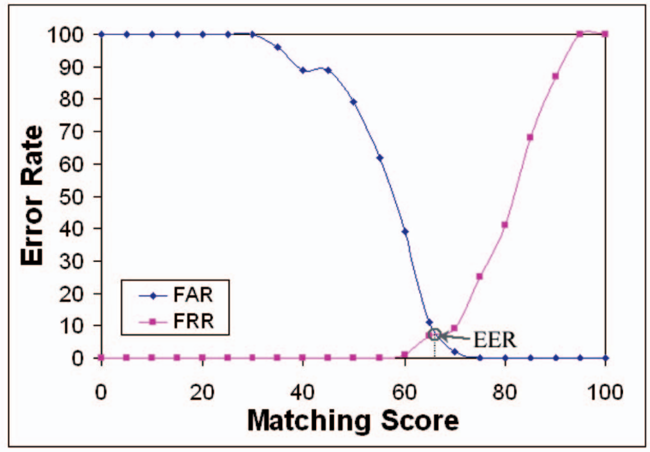

Fig. 19. Plots of FAR and FRR for different values of T_{score}.

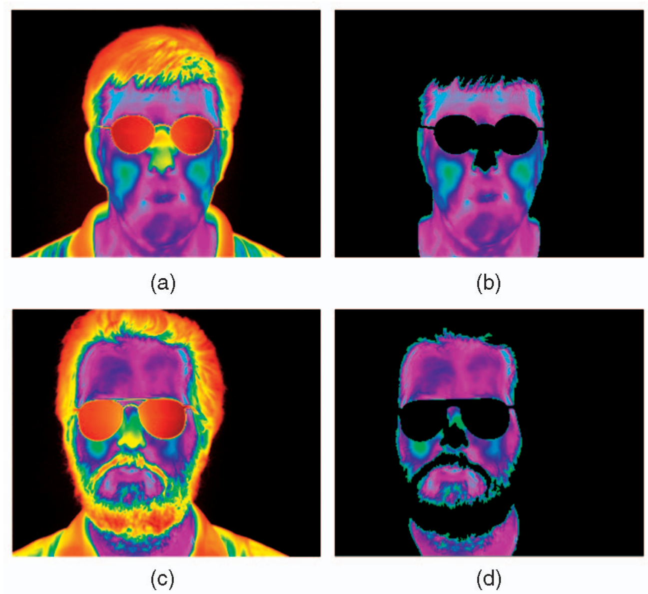

Fig. 20. (a) A thermal facial image with glasses and (b) the result of segmentation. (c) A thermal facial image with facial hair and glasses and (d) the result of segmentation.

and temporal), but this is only a qualitative assessment. Occasionally, the algorithm is fooled by areas of high contrast (e.g., hairline and skin) and reports them as vascular contours. Most of these problems are corrected during postprocessing, but some fake vascular contours remain and participate in the matching process with deleterious effects. The current method also fails to take into account nonlinearities in the deformation of the vascular network. Finally, the present method features a simplistic threshold-based classification algorithm that provides binary and not probabilistic decisions. Our ongoing work is addressing all these issues.

As with most methods, this method also has some operational limitations. As such, we identified the presence of glasses and thick facial hair, as well as substantial perspiration, which may be the result of exertion of heat. Substantial perspiration introduces a nonlinear shift in the thermal facial map that the current feature extraction mechanism cannot handle well.

It is a credit to the physiological framework that, despite the deficiencies of the current methodology, the performance is good in two nontrivial databases in terms of size and difficulty (University of Houston and University of Notre Dame). It is an indication that the method is aided by the natural uniqueness and constancy of the feature space.

Acknowledgments

The authors would like to thank the University of Notre Dame for kindly providing us IR images acquired during different sessions. They would also like to thank Chinmay Manohar from Mayo Clinic and Dr. Jay Murthy from the University of Texas Medical School for their valuable assistance. This research was supported mainly by US National Science Foundation Grant DUE-0313880 in "Collaborative Research: Capacity Expansion in Information Assurance" and NSF Grant IIS-0414754 in "Interacting with Human Physiology." It

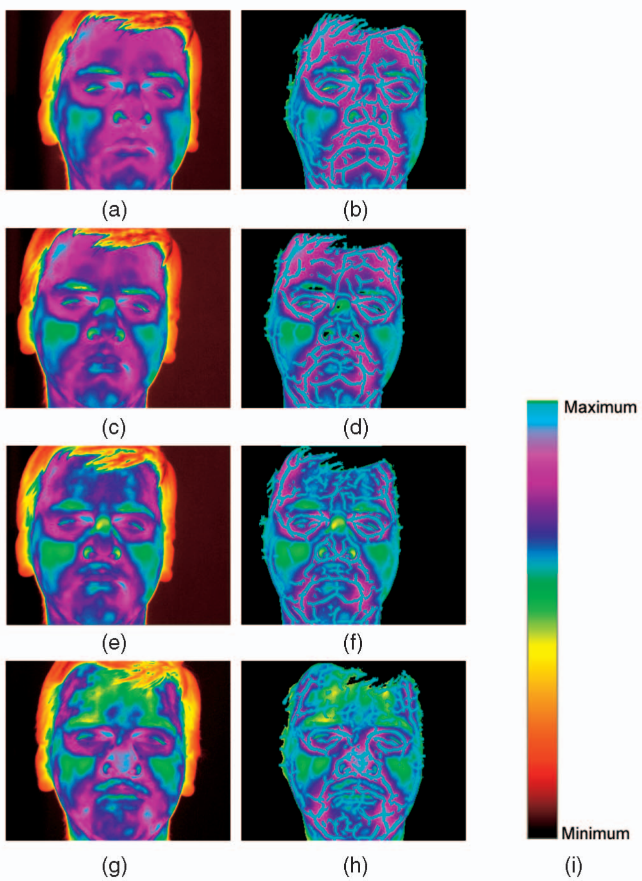

Fig. 21. Effect of perspiration on feature extraction. A thermal facial image of a subject (a) at rest, (c) after 1 minute of rigorous walking, (e) after 5 minutes of rigorous walking, and (g) after 5 minutes of rigorous jogging. (b), (d), (f), and (h) Corresponding vascular network maps. (i) Color map used to visualize temperature values.

was also supported in part by a University Affiliates Grant from Honeywell International in "Biomedical Imaging." The views expressed in this paper do not necessarily represent the views of the funding agencies.

REFERENCES

[1] A. Jain, R. Bolle, and S. Pankanti, *Biometrics: Personal Identification in Networked Society,* first ed. Kluwer Academic, 1999.

[2] W. Zhao, R. Chellappa, P.J. Phillips, and A. Rosenfeld, "Face Recognition: A Literature Survey," *ACM Computing Surveys,* vol. 35, no. 4, pp. 399-458, Dec. 2003.

[3] I. Pavlidis and P. Symosek, "The Imaging Issue in an Automatic Face/Disguise Detection System," *Proc. IEEE Workshop Computer Vision Beyond the Visible Spectrum: Methods and Applications,* pp. 15-24, June 2000.

[4] S. Zhao and R.R. Grigat, "An Automatic Face Recognition System in the Near Infrared Spectrum," *Proc. Fourth Int'l Conf. Machine Learning and Data Mining in Pattern Recognition,* pp. 437-444, July 2005.

[5] X. Zou, J. Kittler, and K. Messer, "Face Recognition Using Active Near-IR Illumination," *Proc. 2005 British Machine Vision Conf.,* Sept. 2005.

[6] S.Z. Li, L. Zhang, S. Liao, X. Zhu, R. Chu, M. Ao, and R. He, "A Near-Infrared Image Based Face Recognition System," *Proc. Seventh Int'l Conf. Automatic Face Gesture Recognition,* pp. 455-460, 2006.

[7] F. Prokoski, "History, Current Status, and Future of Infrared Identification," *Proc. IEEE Workshop Computer Vision beyond the Visible Spectrum: Methods and Applications,* pp. 5-14, June 2000.

[8] D.A. Socolinsky and A. Selinger, "A Comparative Analysis of Face Recognition Performance with Visible and Thermal Infrared Imagery," *Proc. 16th Int'l Conf. Pattern Recognition,* vol. 4, pp. 217-222, 2002.

[9] J. Wilder et al., "Comparison of Visible and Infrared Imagery for Face Recognition," *Proc. Second Int'l Conf. Automatic Face and Gesture Recognition,* pp. 182-187, Oct. 1996.

[10] D.A. Socolinsky, L.B. Wolff, J.D. Neuheisel, and C.K. Eveland, "Illumination Invariant Face Recognition Using Thermal Infrared Imagery," *Proc. IEEE CS Conf. Computer Vision and Pattern Recognition,* vol. 1, pp. 527-534, 2001.

[11] A. Selinger and D.A. Socolinsky, "Face Recognition in the Dark," *Proc. Joint IEEE Workshop Object Tracking and Classification beyond the Visible Spectrum,* June 2004.

[12] R. Cutler, *Face Recognition Using Infrared Images and Eigenfaces,* cs.umd.edu/rgc/face/face.htm, 1996.

[13] X. Chen, P.J. Flynn, and K.W. Bowyer, "PCA-Based Face Recognition in Infrared Imagery: Baseline and Comparative Studies," *Proc. IEEE Int'l Workshop Analysis and Modeling of Faces and Gestures,* pp. 127-134, Oct. 2003.

[14] A. Srivastava and X. Liu, "Statistical Hypothesis Pruning for Recognizing Faces from Infrared Images," *J. Image and Vision Computing,* vol. 21, no. 7, pp. 651-661, 2003.

[15] P. Buddharaju, I. Pavlidis, and I. Kakadiaris, "Face Recognition in the Thermal Infrared Spectrum," *Proc. Joint IEEE Workshop Object Tracking and Classification beyond the Visible Spectrum,* June 2004.

[16] J. Heo, S.G. Kong, B.R. Abidi, and M.A. Abidi, "Fusion of Visual and Thermal Signatures with Eyeglass Removal for Robust Face Recognition," *Proc. Joint IEEE Workshop Object Tracking and Classification beyond the Visible Spectrum,* June 2004.

[17] A. Gyaourova, G. Bebis, and I. Pavlidis, "Fusion of Infrared and Visible Images for Face Recognition," *Proc. Eighth European Conf. Computer Vision,* May 2004.

[18] D.A. Socolinsky and A. Selinger, "Thermal Face Recognition in an Operational Scenario," *Proc. IEEE CS Conf. Computer Vision and Pattern Recognition,* vol. 2, pp. 1012-1019, June 2004.

[19] J.-G. Wang, E. Sung, and R. Venkateswarlu, "Registration of Infrared and Visible-Spectrum Imagery for Face Recognition," *Proc. Sixth IEEE Int'l Conf. Automatic Face and Gesture Recognition,* pp. 638-644, May 2004.

[20] X. Chen, P. Flynn, and K. Bowyer, "IR and Visible Light Face Recognition," *Computer Vision and Image Understanding,* vol. 99, no. 3, pp. 332-358, Sept. 2005.

[21] S.G. Kong, J. Heo, B.R. Abidi, J. Paik, and M.A. Abidi, "Recent Advances in Visual and Infrared Face Recognition—A Review," *Computer Vision and Image Understanding,* vol. 97, no. 1, pp. 103-135, Jan. 2005.

[22] D. Zhuang, Y. Ding, and K. Wang, "A Study of Hand Vein Recognition Method," *Proc. IEEE Int'l Conf. Mechatronics and Automation,* vol. 4, pp. 2106-2110, July 2005.

[23] Snowflake Technologies, www.luminetx.com, 2007.

[24] F.J. Prokoski and R. Riedel, "Infrared Identification of Faces and Body Parts," *BIOMETRICS: Personal Identification in Networked Society,* A.K. Jain, R. Bolle, and S. Pankati, eds., chapter 9. Kluwer Academic, 1998.

[25] P. Buddharaju, I.T. Pavlidis, and P. Tsiamyrtzis, "Physiology-Based Face Recognition," *Proc. IEEE Conf. Advanced Video and Signal-Based Surveillance,* pp. 354-359, Sept. 2005.

[26] P. Buddharaju, I.T. Pavlidis, and P. Tsiamyrtzis, "Pose-Invariant Physiological Face Recognition in the Thermal Infrared Spectrum," *Proc. 2006 IEEE Conf. Computer Vision and Pattern Recognition,* pp. 53-60, June 2006.

[27] B.J. Moxham, C. Kirsh, B. Berkovitz, G. Alusi, and T. Cheeseman, *Interactive Head and Neck (CD-ROM).* Primal Pictures, Dec. 2002.

[28] C. Manohar, "Extraction of Superficial Vasculature in Thermal Imaging," master's thesis, Dept. Electrical Eng., Univ. of Houston, Houston, Texas, Dec. 2004.

[29] Y.A. Pinar and F. Govsa, "Anatomy of the Superficial Temporal Artery and Its Branches: Its Importance for Surgery," *Surgical and Radiologic Anatomy (SRA),* vol. 28, no. 3, pp. 248-253, June 2006.

[30] L.B. Rowell, "Reflex Control of Cutaneous Vasculature," *J. Investigative Dermatology,* vol. 69, no. 1, pp. 154-166, July 1977.

[31] S. De Geef, P. Claes, D. Vandermeulen, W. Mollemans, and P.G. Willems, "Large-Scale In-Vivo Caucasian Facial Soft Tissue Thickness Database for Craniofacial Reconstruction," *Forensic Science,* vol. 159, no. 1, pp. S126-S146, May 2006.

[32] "Biometrics Database Distribution," The Computer Vision Laboratory, Univ. of Notre Dame, http://www.nd.edu/cvrl/, 2002.
[33] S. Pankanti, S. Prabhakar, and A.K. Jain, "On the Individuality of Fingerprints," *IEEE Trans. Pattern Analysis and Machine Intelligence,* vol. 24, no. 8, pp. 1010-1025, Aug. 2002.
[34] I. Pavlidis, P. Tsiamyrtzis, C. Manohar, and P. Buddharaju, "Biometrics: Face Recognition in Thermal Infrared," *Biomedical Eng. Handbook,* CRC Press, Feb. 2006.
[35] M. Garbey, A. Merla, and I. Pavlidis, "Estimation of Blood Flow Speed and Vessel Location from Thermal Video," *Proc. 2004 IEEE CS Conf. Computer Vision and Pattern Recognition,* vol. 1, pp. 356-363, June 2004.
[36] D. Maltoni, D. Maio, A.K. Jain, and S. Prabhakar, *Handbook of Fingerprint Recognition.* Springer, June 2003.
[37] M.D. Almeida Oliveira and N.J. Leite, "Reconnection of Fingerprint Ridges Based on Morphological Operators and Multiscale Directional Information," *Proc. 17th Brazilian Symp. Computer Graphics and Image Processing,* pp. 122-129, Oct. 2004.
[38] B.K. Jang and R.T. Chin, "One-Pass Parallel Thinning: Analysis, Properties, and Quantitative Evaluation," *IEEE Trans. Pattern Analysis and Machine Intelligence,* vol. 14, no. 11, pp. 1129-1140, Nov. 1992.
[39] Z. Yang, H. Ai, B. Wu, S. Lao, and L. Cai, "Face Pose Estimation and Its Application in Video Shot Selection," *Proc. 17th Int'l Conf. Pattern Recognition,* vol. 1, pp. 322-325, Aug. 2004.
[40] Y. Li, S. Gong, J. Sherrah, and H. Liddell, "Support Vector Machine Based Multi-View Face Detection and Recognition," *Image and Vision Computing,* vol. 22, no. 5, pp. 413-427, 2004.
[41] S. Yang and I.M. Verbauwhede, "A Secure Fingerprint Matching Technique," *Proc. 2003 ACM SIGMM Workshop Biometrics Methods and Applications,* pp. 89-94, 2003.
[42] X. Jiang and W.-Y. Yau, "Fingerprint Minutiae Matching Based on the Local and Global Structures," *Proc. 15th Int'l Conf. Pattern Recognition,* vol. 2, pp. 1038-1041, Sept. 2000.
[43] "Flir Systems," http://www.flir.com, 2007.
[44] D.A. Socolinsky and A. Selinger, "Thermal Face Recognition Over Time," *Proc. 17th Int'l Conf. Pattern Recognition,* vol. 4, pp. 23-26, Aug. 2004.
[45] P.J. Phillips, H. Moon, S.A. Rizvi, and P.J. Rauss, "The Feret Evaluation Methodology for Face-Recognition Algorithms," *IEEE Trans. Pattern Analysis and Machine Intelligence,* vol. 22, no. 10, pp. 1090-1104, Oct. 2000.

Pradeep Buddharaju received the BTech degree from Jawaharlal Nehru Technological University (JNTU), Andhra Pradesh, India, and the MS degree from the University of Houston, both in computer science. He is currently a PhD candidate at the Computer Science Department, University of Houston. His research interests include biometric authentication, security, surveillance, pattern recognition, and computer vision. He worked as a summer research intern at Honeywell Laboratories in 2004, 2005, and 2006. He is the recipient of the Motorola Outstanding Paper Award at the Third International Summer School on Biometrics, Alghero, Italy, in 2006. He also received the Best Teaching Assistant Award from the Department of Computer Science, University of Houston, in 2004.

Ioannis T. Pavlidis received the BS degree in electrical engineering from Democritus University in Greece, the MS degree in robotics from the Imperial College of the University of London, and the PhD and MS degrees in computer science from the University of Minnesota. He joined the Computer Science Department, University of Houston, in September 2002, where he is currently the Eckhard Pfeiffer Professor and director of the Computational Physiology Laboratory. He also serves as an associate editor of *Pattern Analysis and Applications* (Springer) and has chaired numerous major IEEE conferences. His current research interests include computational medicine, where he is charting new territory. He has developed a series of methods to compute vital signs of subjects in an automated, contact-free, and passive manner. This new technology has found widespread applications in computational psychology and is expected to find additional applications in preventive medicine. The quantification of stress, in particular, through the computation of periorbital blood perfusion, is his most well-known piece of research. It is this research that established him as one of the founders of modern lie detection technology. He is a Fulbright Fellow, a senior member of the IEEE, and a member of the ACM.

Panagiotis Tsiamyrtzis received the BS degree in mathematics from the Aristotle University of Thessaloniki, Greece. He obtained the MS and PhD degrees in statistics from the University of Minnesota, where he served as a visiting faculty member in the School of Statistics in Fall 2000. In 2004, he joined the Department of Statistics, Athens University of Economics and Business, where he is currently a lecturer. His research interests include computer vision, statistical process control, and applications of Bayesian statistics. He was the recipient of the Best Student Paper Award and Best Contributed Paper in the Joint Statistical Meetings 2000 of the Risk Analysis Section of the American Statistical Association.

Mike Bazakos received the BS degree in mathematics from the National University of Athens and the MS degree in applied mathematics from the University of Minnesota. He was a principal investigator in several military and civilian surveillance projects. He has cochaired numerous government and academic conferences. He is a senior fellow at the Honeywell Advanced Technology Laboratories (ATL). His main research interests include image processing, pattern recognition, and computer vision systems. He holds six patents and coauthored more than 20 publications. He is also a three-time recipient of the highest Technology Achievement Award at Honeywell Laboratories.